Research Article

Computational Analysis Of 2d Aerospike Nozzle With Base Bleed At Different Altitudes

Santhosh Kumar[a*], Mouli Bhaskar[b], Manur Gautam[c], Bhanu Prakash[d], Sarath Kumar[e]

[a,b,c,d] Student, School of Aeronautical Sciences, Hindustan Institute of Technology & Science, Chennai, India
[e] Assistant Professor, School of Aeronautical Sciences, Hindustan Institute of Technology & Science, Chennai, India

Article History: Received: 10 January 2021; Revised: 12 February 2021; Accepted: 27 March 2021; Published online: 28 April 2021

Abstract:
In the present-day scenario, several nozzles are being developed to achieve better efficiency. Among them, the aerospike is one such nozzle. The aerospike nozzles are yet to be utilized in the aerospace sector but are believed to exhibit better performance than the conventional bell-shaped nozzles that are currently in service. The geometry of the aerospike nozzle enables it to adjust to its environment by modifying its outer jet boundary thus, making it more efficient than the other types of nozzles.
Simple approximation method is used to get the coordinates of the nozzle contour using MATLAB. To compare the performance characteristics, both full and truncated spike nozzles were designed using SOLIDWORKS. In order to improve the performance of the truncated aerospike nozzles, they are provided with base bleeds. The flow behaviour was analysed using Computational Fluid Dynamics (CFD) software – ANSYS. These designs were simulated for different pressure outlet conditions, to compare the performance of full length, truncated spike with and without base bleed, at different altitudes.

Keywords: aerospike nozzle, plug, truncation, cowl-lip, barrel shock, CFD.

Nomenclature:

μ Mach Angle
ν Prandtl – Meyer function
l Length of the Characteristic line
A_R Nozzle Expansion ratio
α Angle between characteristic line and sonic flow
λ $\frac{l}{l_t}$,Non-dimensional length for plane nozzle
S Surface area
A_t Nozzle throat area
A_e Nozzle exit area
η_b Non–Dimensional base radius
ξ $\frac{l}{r_e}$, Non-Dimensional length of axisymmetric nozzle
M Mach Number
γ Ratio of specific heats

Subscripts

t throat
e exit area
b base

Introduction:

Over the past few decades, mankind has shown immense potential in the field of aerospace. A key concept in the exploration of space is the advancement in aerospace technology. In an aircraft, a nozzle plays a crucial role across which the potential energy of the fluid is converted into kinetic energy, thus providing sufficient space for the expansion of gases. Nozzles are mechanical devices that control the flow and direction of exhaust gases [1]. Different types of nozzles are used depending upon the requirement and operating conditions. Presently a Convergent-Divergent (CD) nozzle is used predominantly for space missions. The CD nozzle has its drawbacks. A typical CD nozzle requires huge space to fit into the engine and the fluid flow across the nozzle tends to separate at the walls, thus reducing its performance. One of the nozzles that are being developed to overcome such problems is the Aerospike nozzles. Aerospike nozzles are altitude compensating nozzles with shortened nozzle length for the same or increased performance. Aerospike nozzles are often referred to as an Inside-out bell-shaped nozzle [2-3]. This nozzle was developed in the view of Single Stage to Orbit (SSTO) vehicles.
While operating CD nozzles at low altitudes, if the exit pressure is lesser than the ambient pressure, the flow gets radially compressed inwards resulting in the separation of flow at walls of nozzle and thus decreasing the efficiency [3-4]. At higher altitudes, the ambient pressure will be very low which results in the flow expanding past the nozzle. In an aerospike nozzle, the expansion process will begin at a point on the outer edge of the annulus known as the cowl-lip. The combusted gases are directed towards the axis of the nozzle [4]. The gases exiting from the spike are not enclosed by an external boundary. If an aerospike nozzle is operated in an over-expanded mode, the flow gets imparted on the spike and thus maintains its efficiency. If an aerospike nozzle is operated in an under-expanded

mode, since the flow is not enclosed by any boundary, the thrust gets imparted on the centre spike and maintains its efficiency. As there is an increase in altitude, the aerospike nozzle maintains a better aerodynamic efficiency throughout the trajectory. Because of this reason, it is also termed as an Altitude-Compensating nozzle. Aerospike nozzles produce a higher thrust efficiency and better average specific impulse since it makes better use of the base area. Up to 25% of the fuel is saved if a vehicle is operated with an aerospike nozzle at low altitudes. Overall performance of the aerospike nozzle is better than the conventional bell-shaped (CD) nozzle [4].

The main drawback of an aerospike nozzle is its unsustainability at high temperatures. Since the hot gases after the combustion reach the nozzle at very high temperatures, the sharp edge of the nozzle (spike) cannot resist. Truncation of the spike has been done to overcome this issue. In truncated aerospike nozzles, the specified length of the spike will be removed which results in a flat base [5-7]. Due to high ambient pressure at low altitudes, the gases at the exhaust remain close to the nozzle wall and it is said to be operating in open-wake conditions as shown in Fig. 1a. At high altitudes, the ambient pressure will be very low which might cause an under expansion. But due to the formation of barrel shock and trailing shock within the exhaust flow, it retains a column shape (which forms at the design altitude) under the close wake condition as shown in Fig. 1b.

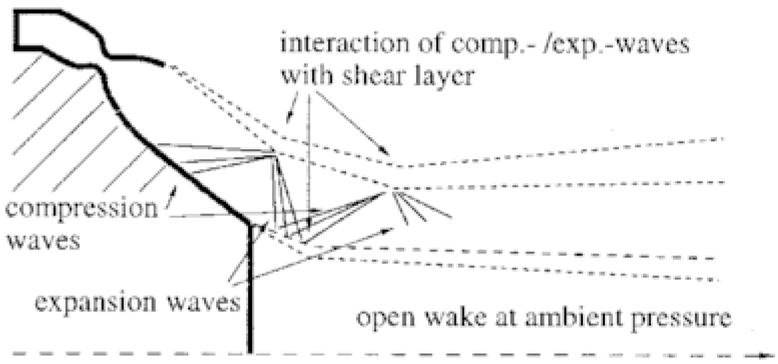

Fig. 1a Flow phenomenon of an over-expanded truncated aerospike nozzle**.**

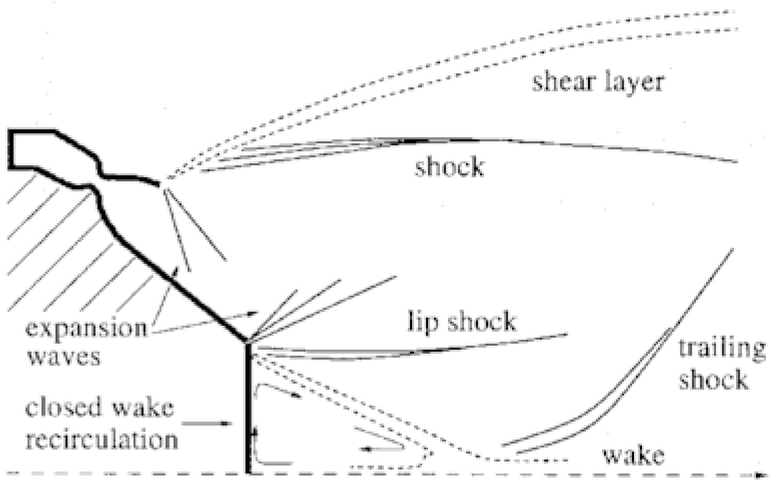

Fig. 1b Flow phenomenon of an under-expanded truncated aerospike nozzle.

As the altitude increases, there will be a loss in performance for a truncated aerospike nozzle. These losses can be balanced by introducing base bleed. From the base region, a secondary flow is implemented [4].

This paper compares the performances of full-length aerospike nozzle and truncated aerospike included with base bleed at different altitudes. Mach contours of all the nozzles and the pressure plots for different truncations of the nozzle were discussed.

Methodology

1. Nozzle Contour Design

The technique used to design the nozzle contour is the approximation method which is based on the method of characteristics. The method of characteristics takes the inviscid assumption for devising the governing equations. The method used in this paper is similar to the one used by Angelino [8].

Along the characteristic lines, the derivatives blow up to be of an indeterminate form and may be discontinuous. The contour is designed by considering a point from where the characteristic lines originate. This point acts as the tip of the cowl and its position is user-defined. The characteristic line corresponding to the throat of the nozzle is referred to as a sonic line since the Mach number at the throat is unity. The characteristic lines originating from the tip of the cowl are inclined at an angle with respect to the sonic flow and are given by, α = μ - ν, where μ and ν correspond to the Mach angle and Prandtl Meyer function respectively [9].

The value of μ is given by, $\mu = \arcsin\left(\frac{1}{M}\right)$, and

the Prandtl Meyer expansion function is given by

$$\nu(M) = \sqrt{\frac{\gamma+1}{\gamma-1}}\; arctan\sqrt{\left(\frac{\gamma-1}{\gamma+1}\right)(M^2-1)} - \; arctan\sqrt{M^2-1}$$

The characteristic lines cross the required contour boundary at a distance *l* from the cowl lip. The distance *l* can be computed by using the continuity equation

$$\frac{l}{l_t} = \left(\frac{A}{sin\mu}\right)\left(\frac{1}{A_t}\right) \quad (1)$$

where A is equal to the area normal to the velocity vector and l_t is defined as the distance between the nozzle contour boundary and cowl lip. The above equation can also be written as

$$\lambda = (A\_R) * M \quad (2)$$

where A_R is defined as the nozzle expansion ratio.

In the above set of formulae, the Mach number values are to be varied in ascending order starting from 1 to the desired exit Mach number [8]. For each value of the Mach number, the values of μ, ν, α, and area ratio are recorded. In the below figure [8], a sonic flow is present at the throat of the nozzle. The characteristic lines originating from the cowl lip are straight and follow the two-dimensional law.

From the figure we have,

$$S = 2\pi\, \frac{r_e + r}{2}\, \frac{r_e - r}{sin\alpha} \quad (3)$$

Where *S* is defined as the surface area crossed by the flow.

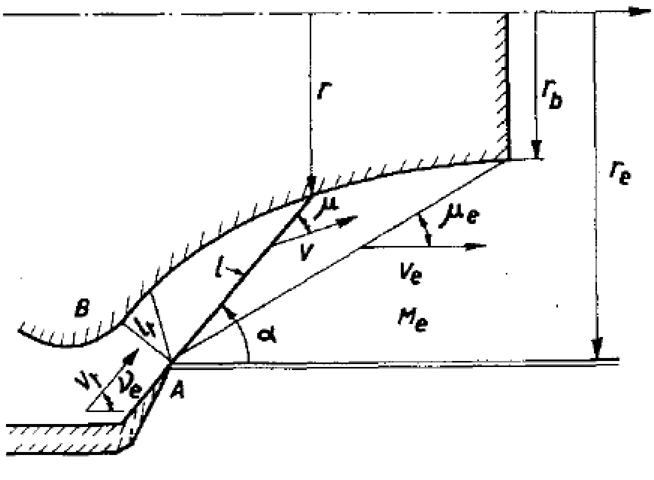

Fig. 2 Schematic diagram of two-dimensional Aerospike nozzle

The velocity vector makes an angle μ with the surface, thus the actual area becomes

$$A = S\, sin\mu = \frac{r_e - r}{M\, sin\mu} \quad (4)$$

Furthermore, the length of the characteristic line is given by

$$l = \frac{r_e - r}{sin\alpha} \quad (5)$$

The exit area of the nozzle is given by

$$A_e = \pi(r_e^2 - r_b^2)$$

For the case of full truncation aerospike nozzle, r_b will be equal to zero.

Keeping equation (5) in mind, equation (4) can be rewritten as

$$l = \frac{r_e - \sqrt{r_e^2 - \frac{A\,M\,sin\alpha}{\pi}}}{sin\alpha} \quad (6)$$

The above equation can be non-dimensionalized with respect to the exit radius of the spike. Thus, the transformed equation becomes

$$\xi = \frac{l}{r_e} = \frac{1-(1-(A\_R_i(1-\eta_b^2)\; M\; \frac{sin\alpha}{A\_R}))}{sin\alpha} \quad (7)$$

Here η_b is defined as the non-dimensional base radius [8].

With the help of the above set of relations, each coordinate of the nozzle contour is computed independently, thus providing greater accuracy.

MATLAB code for nozzles is prepared with the help of the thesis [10] and analysis has been carried out for different truncations. The amount of truncation is mentioned in the code itself. In this paper length truncation of aerospike nozzle has been carried out for 15%, 30% along with base bleeds. The input parameters for geometry are taken from [10], and the ratio of specific heats is chosen for Liquid Oxygen & Liquid Hydrogen based on the mixture ratio [11]. Input parameters for design are:

- The ratio of specific heats: 1.203
- Area ratio: 6.8214
- Tube diameter: 3.2036

The geometry is developed using SOLIDWORKS from the generated MATLAB code. The analysis is done using the CFD software Ansys Student. The outlet and far-field distance from the tip of the plug are 10 & 5 times the exit diameter to the X & Y-axis respectively. Since the nozzle flow is axisymmetric and to reduce the computational time, the upper half of the nozzle is only designed for analysis. Fig. 3 shows the spike contour of a full-length nozzle generated from code.

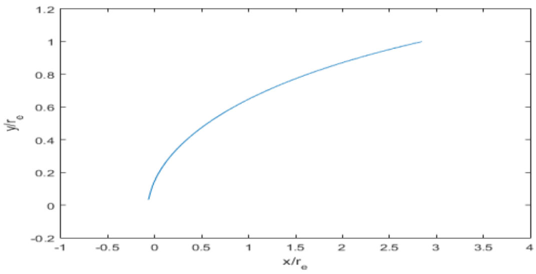

Fig. 3 Plug contour generated from MATLAB

2. Grid Generation

To facilitate different initial conditions in each region, the domain has been divided into 4 regions. Multizone Quad/tri meshing is used to the entire domain to improve the overall quality of the mesh [12]. The intensity of the grid is more near the plug wall to capture the variable gradients. A grid independence study was done and found the number of cells to be around 40000. The meshing is done accordingly for all designs.

3. Fluent setup

The flow is assumed to be a steady, viscous, and ideal gas. The density-based model with the K-Omega SST turbulence method is used for the better prediction of flow behaviour. The boundary conditions for various regions are taken as shown in table 1. For base bleed, a secondary inlet is provided which is of the velocity-type. The magnitude of fluid velocity at the secondary inlet is taken as 80 m/s. Since the analysis is being done for cold flow, the outlet, far-field and the chamber temperatures are maintained at 300 K.

The coupled implicit linearization with second-order upwind discretization is used for the solution of governing equations [13]. Courant number (CFL number) has been set to 1 for all cases.

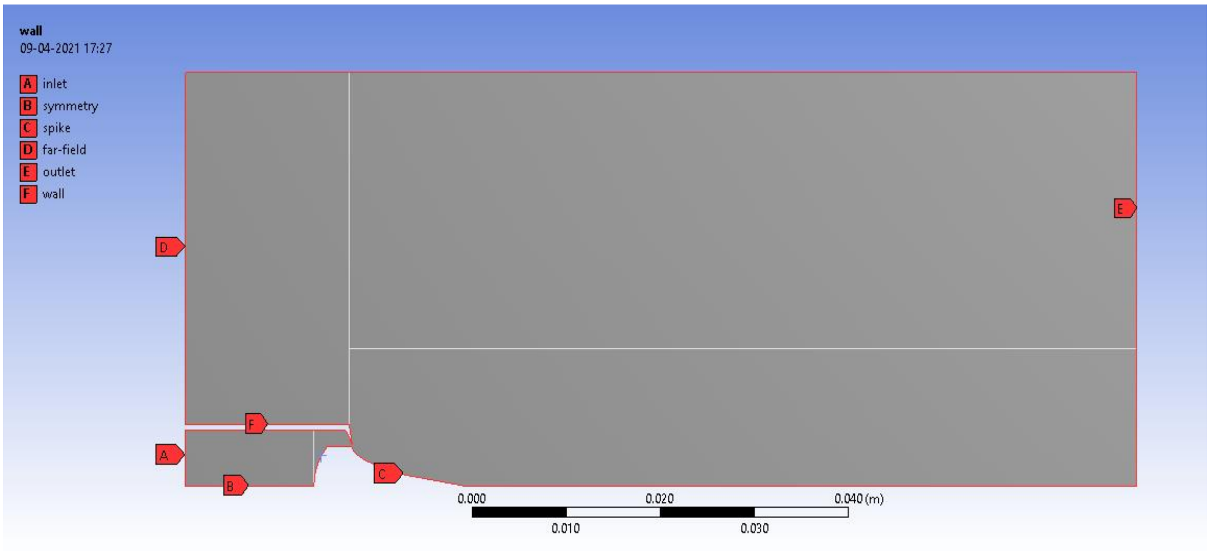

Fig. 4 Solution domain and regions

Table 1: Boundary conditions

Altitude(m)	Chamber Pressure (Pa)	Pressure Far-field (Pa)	Outlet Pressure (Pa)
0	6079500	101325	101325
10400	6079500	24856.4	24856.4
19000	6079500	6410	6410
36000	6079500	509.14	509.14
100000	6079500	1	1

Results & Discussion:

In this section, the performance analysis of different nozzles is compared through Mach contours and static pressure plots at various altitudes.

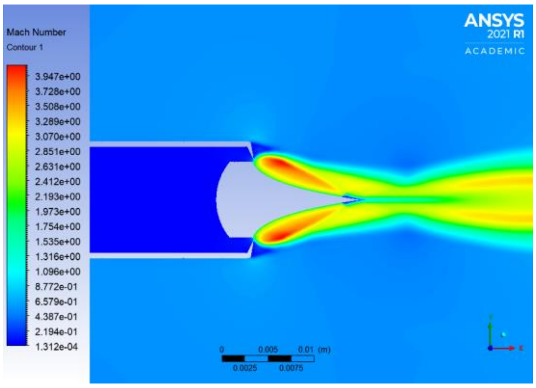

(a) At Sea level

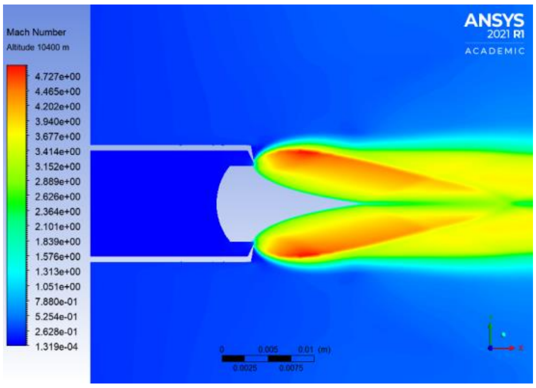

(b) At 10400 m

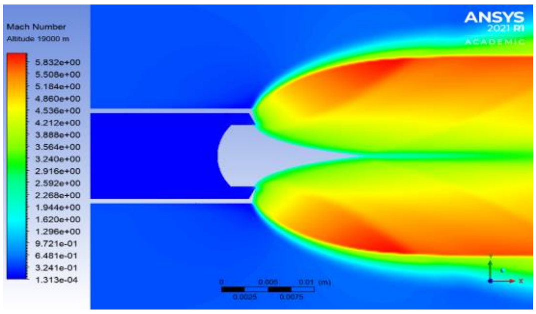

(c) At 19000 m

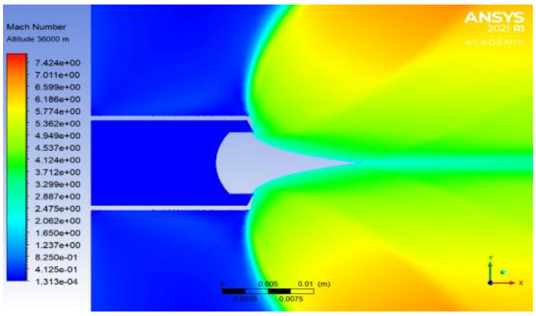

(d) At 36000 m

(e) At 100000 m

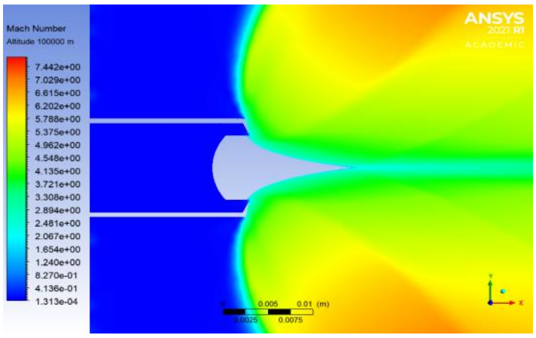

Fig. 5 Mach contours of full-length plug nozzle at different altitudes

From the fig. 5, it can be seen that the exhaust fluid undergoes expansion process and bulges outward with the increase in altitude. The exit Mach number at the end of the spike also increases with the increase in altitude. At higher altitudes the expansion waves originating from the cowl-lip causes the flow to encounter a sharp expansion, thus resulting in higher Mach number region.

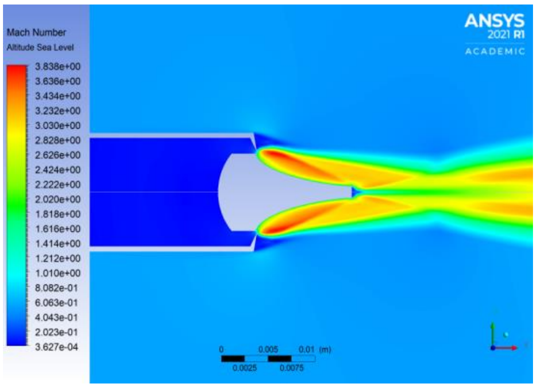

(a) At sea level

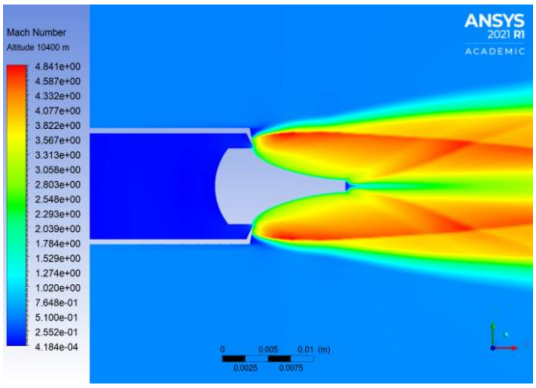

(b) At 10400 m

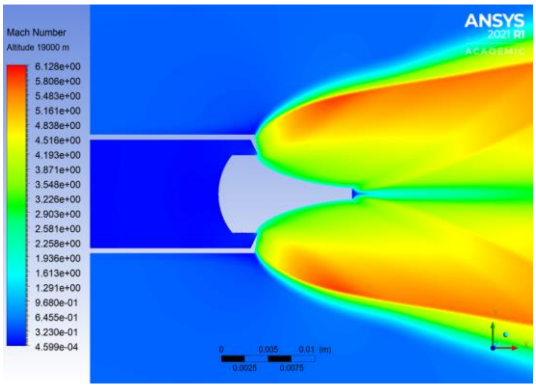

(c) At 19000 m

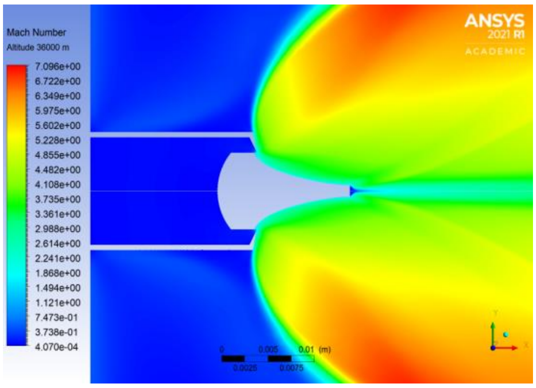

(d) At 36000 m

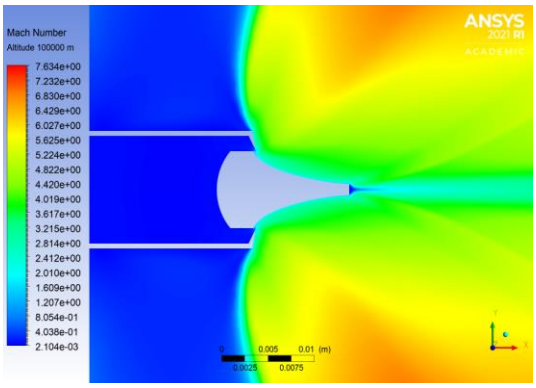

(e) At 100000 m

Fig. 6 Mach contours of 15% truncated plug nozzle at different altitudes

By truncating full length nozzle to 15% it can be observed that the expansion of jet is even stronger due to the truncated portion of the nozzle. The truncation of the spike results in shorter distance and the expansion waves originating from the plug encounters another expansion wave caused by the expansion of the flow at the tip of the truncated portion of the plug. This phenomenon can be observed at higher altitudes i.e., fig. 6.

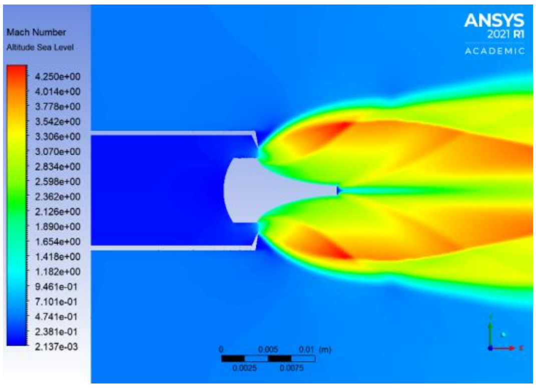

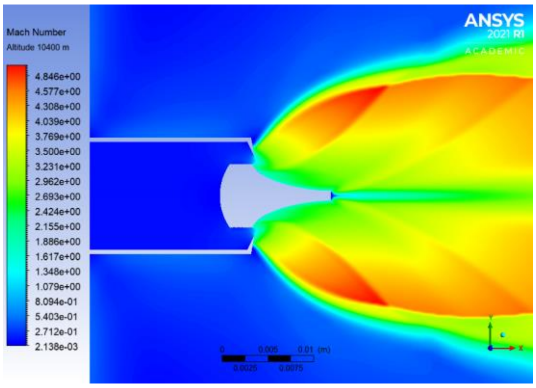

(a) At sea level

(b) At 10400 m

(c) At 19000 m

(d) At 36000 m

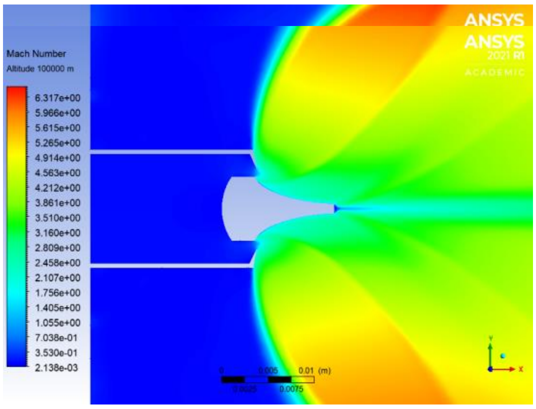

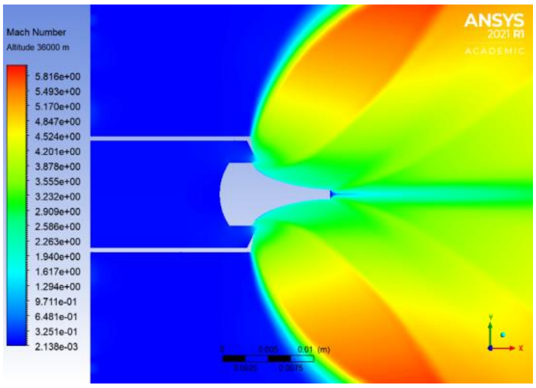

(d) At 100000 m

Fig. 7 Mach contours of 30% truncated plug nozzle at different altitudes

Similar process can be observed for 30% truncated nozzle. Since this truncated portion of nozzle results in even shorter distance, the expansion of jet is even fiercer. The encountering of expansion of the flow at the tip to the originating flow from the plug results in high-Mach number region when compared to 15% truncated nozzle, and can be seen from fig. 7.

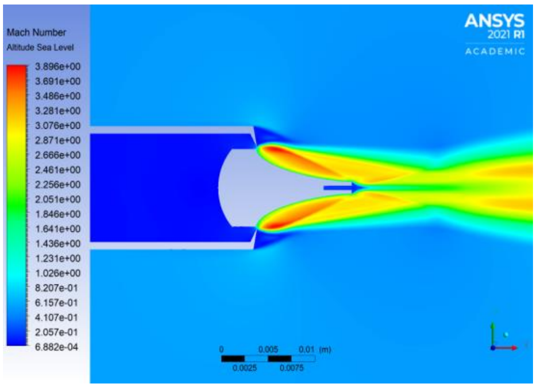

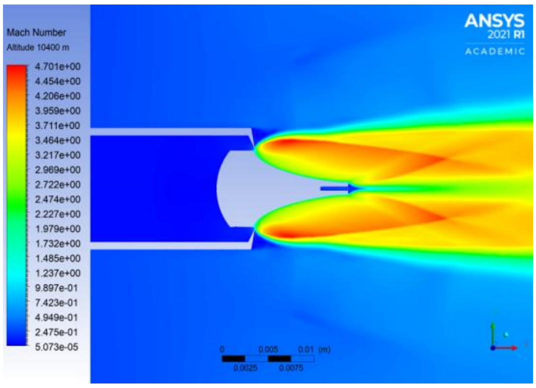

(a) At sea level

(b) At 10400 m

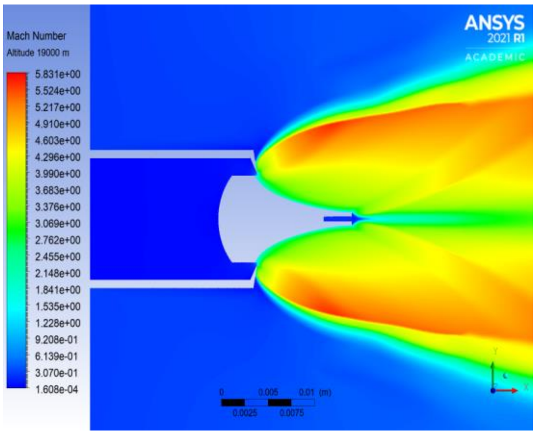

(c) At 19000 m

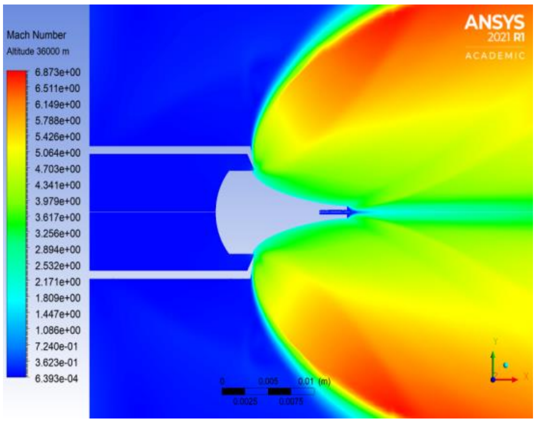

(d) At 36000 m

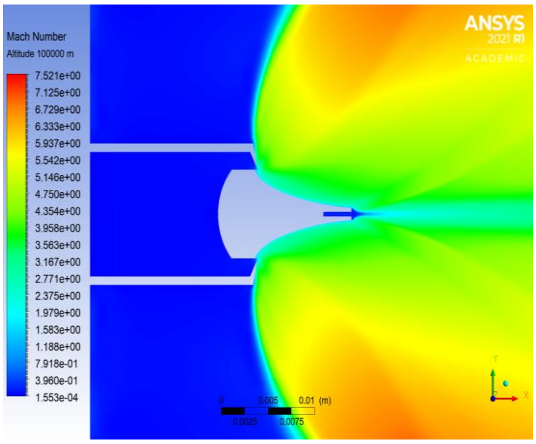

(e) At 100000 m

Fig. 8 Mach contours of 15% truncated plug nozzle with base bleed of velocity 80m/s at different altitudes

The flow structure at the base changes drastically with the introduction of base-bleed, because of the interaction of subsonic and supersonic flows, resulting in a better converged flow in comparison with no base bleed nozzle. These changes can be seen from comparing fig. 8 (a) and fig. 6 (a). The effect of base-bleed is significantly less for higher altitude.

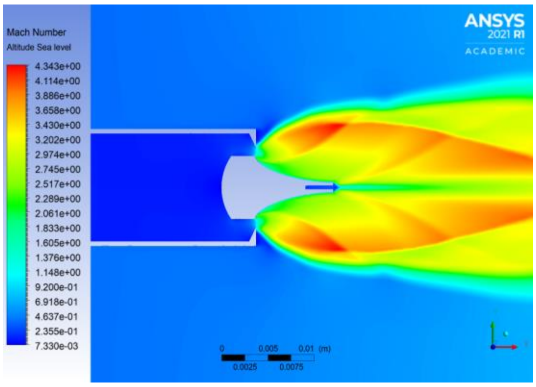

(a) At sea level

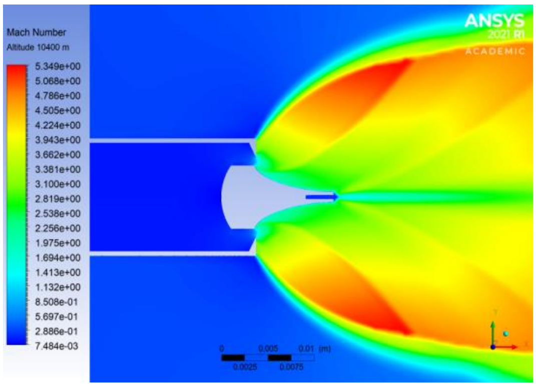

(b) At 10400 m

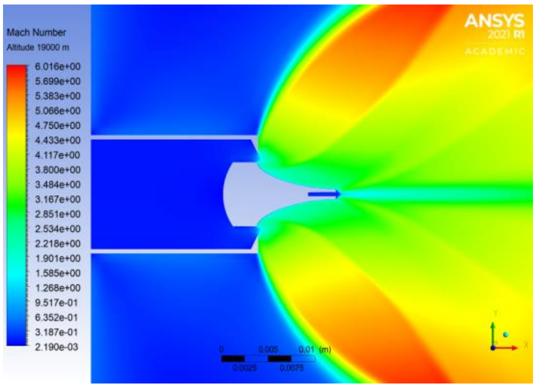

(c) At 19000 m

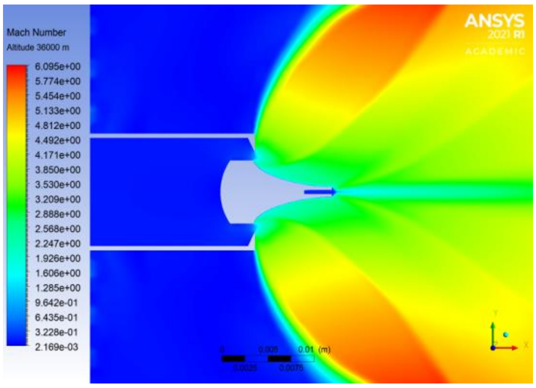

(d) At 36000 m

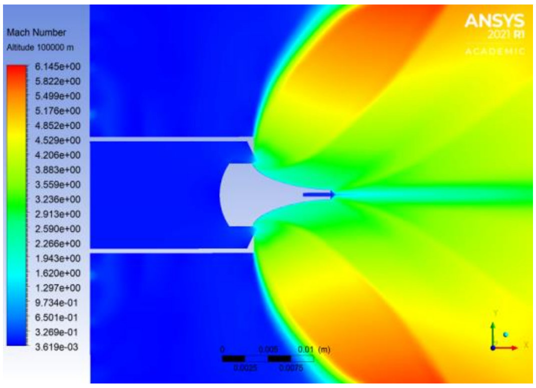

(e) At 100000 m

Fig. 9 Mach contours of 30% truncated plug nozzle with base bleed of velocity 80 m/s at different altitudes

A similar trend is observed for 30% truncated nozzle with base bleed. When compared at the same altitude, with the increase in truncation of the nozzle, the Mach number at the nozzle exit also increases. By introducing the base bleed, the flow recirculation at the flat base is reduced, such that there will not be any sudden pressure drop at the base of the nozzle. From figures 8, 9 & 6,7, it can be seen that the amount of variation in performance with the introduction of the base bleed of velocity 80 m/s is significantly less.

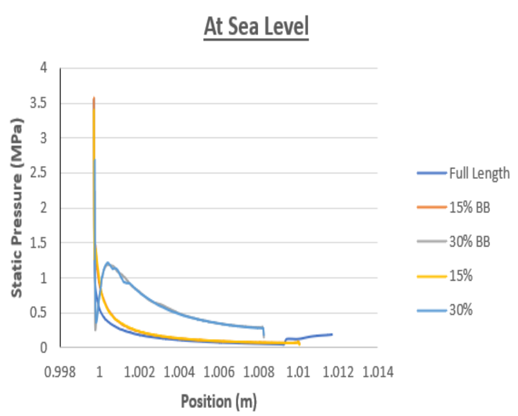

(a) At sea level

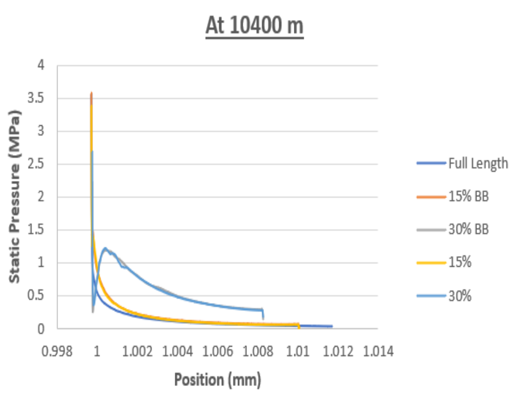

(b) At 10400 m

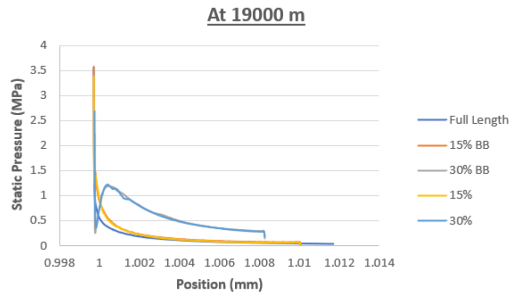

(c) At 19000 m

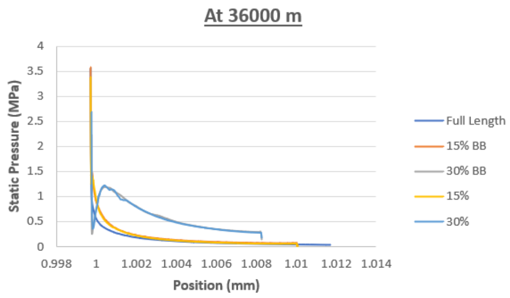

(d) At 36000 m

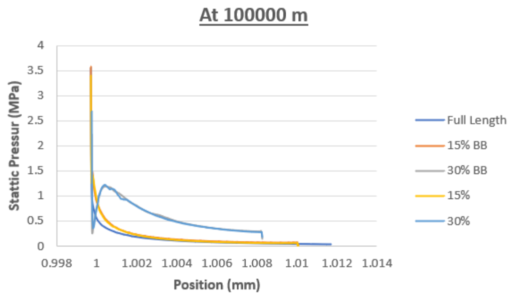

(e) At 100000 m

Fig. 10 Static Pressure change over the spike for different plug truncations at different altitudes

The above figure represents the pressure contours over the spike at different conditions. The flow coming out of the throat experiences a huge loss in static pressure due to strong expansion. It is observed that the static pressure over the spike of the nozzle does not significantly vary with respect to the altitude.

Conclusion:

Flow structure and performance of the truncated nozzles were compared. The static pressure variation over plug is found to be very small with respect to altitude for different truncation ratios. The loss in performance due to under-expansion at different altitudes is compensated by giving length truncation. Truncating the spike gave a significant increase in Mach number at the exit of the nozzle, which can be observed for 15% and 30% truncation.

It is found that introducing lower base bleed velocities has no significant variation in the performance of the nozzle. The higher base bleed velocities may compensate for the loss in thrust/performance due to under-expansion. It is recommended to use truncated nozzles for better performance at higher altitudes of flight.
Based on the studied parameters, it can be concluded that the amount of truncation depends on the flight regime and the propulsive system.

References:

1. Kumar, K. Naveen, et al. "Design and Optimization of Aerospike Nozzles using CFD." *IOP Conference Series: Materials Science and Engineering*. Vol. 247. No. 1. IOP Publishing, 2017.
2. Nair, Prasanth P., Abhilash Suryan, and Heuy Dong Kim. "Study of conical aerospike nozzles with base-bleed and freestream effects." *Journal of Spacecraft and Rockets* 56.4 (2019): 990-1005.
3. Ladeinde, Temitayo, and Hsun Chen. "Performance Comparison of a Full-Length and a Truncated Aerospike Nozzle." *46th AIAA/ASME/SAE/ASEE Joint Propulsion Conference & Exhibit*. 2010.
4. Bui, Trong, et al. "Flight research of an aerospike nozzle using high power solid rockets." *41st AIAA/ASME/SAE/ASEE Joint Propulsion Conference & Exhibit*. 2005.

5. Choudhari, Dipak J., and Uday V. Asolekar. "Efficiency analysis of an aerospike nozzle." *International Journal of Engineering Research and Applications (IJERA) ISSN* (2012): 2248-9622.
6. Ajith, S., et al. "Performance Evaluation of Aerospike Nozzles for Lucrative Thrust Vector Control." *52nd AIAA/SAE/ASEE Joint Propulsion Conference*. 2016.
7. Takahashi, Hidemi, et al. "Aerodynamic characterization of linear aerospike nozzles in off-design flight conditions." *Journal of Propulsion and Power* 31.1 (2015): 204-218.
8. Angelino, Gianfranco. "Approximate method for plug nozzle design." *AIAA Journal* 2.10 (1964): 1834-1835.
9. Korte, J. J., et al. "Multidisciplinary approach to linear Aerospike nozzle design." *Journal of Propulsion and Power* 17.1 (2001): 93-98.
10. Bani, Abdalla Ali. "Design and analysis of an axisymmetric aerospike supersonic micro-nozzle for a refrigerant-based cold-gas propulsion system for small satellites." (2016).
11. http://www.braeunig.us/space/comb-OH.htm
12. Nazarinia, Mehdi, Arash Naghib-Lahouti, and Elhaum Tolouei. "Design and numerical analysis of aerospike nozzles with different plug shapes to compare their performance with a conventional nozzle." *AIAC-11 Eleventh Australian International Aerospace Congress*. 2005.
13. Guide, ANSYS FLUENT User. "Release 14.0, ANSYS." *Inc., USA, November* (2011).